

Combined Thomson Scattering and Laser-Induced Fluorescence for Studying Divertor and X-point Plasmas in Tokamak with Reactor Technologies

E. E. Mukhin^{a, *}, S. Yu. Tolstyakov^a, G. S. Kurskiev^a, N. S. Zhil'tsov^a, A. N. Koval'^a,
V. A. Solovei^b, A. V. Gorbunov^c, A. V. Gorshkov^c, G. M. Asadulin^c, A. F. Kornev^d,
A. M. Makarov^d, D. L. Bogachev^e, N. A. Babinov^a, D. S. Samsonov^a,
A. G. Razdobarin^a, A. N. Bazhenov^a, I. M. Bukreev^a, A. M. Dmitriev^a, D. I. Elets^a,
V. A. Senichenkov^a, I. B. Tereshchenko^a, L. A. Varshavchik^a, I. A. Khodunov^a,
An. P. Chernakov^a, G. V. Marchii^a, K. O. Nikolaenko^a, and N. V. Ermakov^a

^a Ioffe Institute, Russian Academy of Sciences, Saint Petersburg, 194021 Russia

^b Konstantinov Petersburg Nuclear Physics Institute of National Research Center "Kurchatov Institute,"
Gatchina, Leningrad region, 188300 Russia

^c National Research Centre Kurchatov Institute, Moscow, 123098 Russia

^d Lasers and Optical Systems Co. Ltd., Saint Petersburg, 199053 Russia

^e Joint Stock Company "Spectral-Tech," Saint Petersburg, 194223 Russia

*e-mail: e.mukhin@mail.ioffe.ru

Received March 19, 2022; revised May 25, 2022; accepted May 25, 2022

Abstract—Combined Thomson scattering (TS) and laser-induced fluorescence (LIF) diagnostics are being developed. The Thomson scattering and laser-induced fluorescence are laser diagnostics, with joint both probing and collecting optical systems, which are the most complex and expensive parts of the diagnostic systems of large tokamaks, can be combined. Thomson scattering by free electrons is the use-proven diagnostic method for measuring profiles of important parameters of the plasma electron component (electron temperature T_e and electron density n_e), which requires a minimum of model assumptions. Almost all existing tokamaks are equipped with one or more TS systems, and by now, considerable experience has been accumulated in practical methods for implementation of these systems. The use of laser-induced fluorescence for measuring parameters of ion and neutral plasma components is less common, also because it requires knowledge of electron parameters to calculate populations of excited levels. The joint diagnostics of the Thomson scattering and laser-induced fluorescence in divertor plasma will be used to simultaneously measure the plasma parameters necessary for fundamental understanding physics of plasma detachment from divertor plates. These parameters are: the local parameters of plasma electrons (T_e , n_e), ion temperature (T_i) measured from the data on emission of helium ions (HeII), as well as densities of helium atoms ($n_a(\text{He})$) and hydrogen isotopes ($n_a(\text{H}, \text{D}, \text{T})$). The measured parameters make it possible to calculate the following characteristics: (i) the ionization and recombination rates (using the data on T_e , n_e , T_i , and $n_a(\text{H}, \text{D}, \text{T})$); (ii) the friction force of the plasma flow due to collisions with neutral particles (using the data on T_i , n_i (assuming $n_i = n_e$), and $n_a(\text{H}, \text{D}, \text{T})$); and (iii) the pressure of the oncoming plasma flow (using the data on T_e , n_e , T_i , and n_i). The article discusses advantages of combining laser diagnostics and ways of further development of the joint diagnostics, based on the experience of creating similar diagnostics for domestic tokamaks and the similar diagnostics developed for ITER.

Keywords: TRT, Thomson scattering, quasi-stationary discharge, divertor, LIF

DOI: 10.1134/S1063780X22700301

1. INTRODUCTION

An important part of the experimental program for development of the tokamak with reactor technologies will be the scenarios with large heat fluxes through the last closed magnetic surface. The physical limitations on the heat load onto first wall and divertor elements

become the limiting factors. The divertor is the most critical element of any tokamak reactor, since it is exposed to the most intense energy load. That is why in the TRT project, it is necessary to pay attention to studying edge plasma, plasma-wall interaction, research and control of hydrogen recycling, and con-

trol of the regimes with complete or partial plasma detachment from the divertor, with a considerable reduction of heat load onto the divertor plates. The high power density of additional heating in TRT will result in extremely high heat load in the diverter region, increasing the risk of serious accidents. The research program of divertor technologies at TRT involves implementation of gas divertor with a considerable part of the energy carried out along separatrix is reradiated inside the divertor, which should result in a radical decrease in the power density released in the regions where the separatrix meets the divertor plates. The operating regimes of the gas divertor, their optimization and monitoring during operation are of particular importance for protecting the reactor from emergencies. The model of edge and divertor plasmas, as well as of the detachment regime, has not been fully developed. When developing the operating regimes, reliable experimental data on the distributions of electron, ion, and neutral components (T_e , n_e , T_i , n_i , and $n_a(\text{He, H, D, T})$) are required to confirm theoretical models and numerical codes [1].

The rates of reactions involving the electron component (T_e , n_e), such as ionization, recombination and emission, are of great importance in terms of plasma cooling. The parameters of ion component (T_i , n_i) and density of neutral particles ($n_a(\text{He, H, D, T})$) are important when estimating the rates of ion–neutral collisions, which:

1. Considerably contribute to pressure in the upper central part of the divertor (the region of so-called “divertor leg”).

2. Result in cooling of plasma to a temperature of approximately 1 eV, initiating an increase in recombination.

3. Initiate interaction of charged particles as they move in inhomogeneous plasma that leads to the switching of plasma flows from the regime of free flow to the regime of diffusion propagation, making the residence time of electrons and ions in this region sufficient for recombination and cooling due to radiation.

All three phenomena (deceleration, cooling, and recombination) are important in terms of efficient reduction of the heat flux onto the divertor targets. In case of insufficient deceleration, particles of the plasma flow will reach the divertor plates, being insufficiently cooled, and the energy fluxes carried to the divertor plates may cause their destruction.

2. GOALS AND OBJECTIVES OF DIAGNOSTICS IN THE TRT PROJECT

It is proposed to measure the entire set of plasma parameters in the region of X-point, their changes from X-point along separatrix to outer divertor target and along the surface of outer divertor target plate using the joint TS/LIF laser diagnostics [2]. One of the most important tasks of the diagnostics will be to

test model assumptions concerning plasma behavior in the divertor and its detachment from the divertor target plates. Focusing on studies of the outer divertor leg is explained by the fact that complete plasma detachment usually begins on the inner side of divertor and finished on its outer side [3], as well as by complexity of laser measurements in the region of inner leg.

Simultaneous measurements of T_e , n_e , T_i , and n_i parameters and the isotopic ratio for hydrogen isotopes make it possible to describe a set of physical processes that determine the divertor operation, including the following ones:

– Ionization balance and ionization/recombination rates (T_e , n_e , and $n_a(\text{He, H, D, T})$).

– Radiation loss (T_e , n_e , n_i , and $n_a(\text{He, H, D, T})$).

– Forces of friction in plasma flows (T_i , n_i) against the neutral component ($n_a(\text{He, H, D, T})$) at known velocity of relative motion of the plasma components.

– Pressure along outer leg of the divertor (T_e , n_e , T_i , and n_i).

– Isotopic ratios $R_{\text{H/D}} = n_a(\text{H})/n_a(\text{D})$ and $R_{\text{D/T}} = n_a(\text{D})/n_a(\text{T})$.

The objectives of joint TS/LIF laser diagnostics are to measure a set of plasma parameters in accordance with the technical requirements presented in Table 1.

The required spatial resolutions of diagnostics are approximately 30 mm along B-field line in the divertor and ~10 mm across the field lines. The required time resolution of quasi-stationary processes in the divertor is ~100 ms that is determined by time scale close to the lifetime of plasma particles in the TRT divertor. For example, during the L–H transition, fast processes in the ITER divertor plasma [3] require time resolution of approximately 10 ms. In order to obtain useful information during existence of the so-called edge-localized modes (ELM), having complex filamentary structure that is observed in all modern tokamaks (see, for example, [4]), the necessary delay between Thomson scattering pulses should be as low as 10 μs [5]. To ensure measurements of fast transient processes, the

Table 1. Technical requirements for the TS/LIF diagnostics

Parameter	Range	Error
n_e [m^{-3}]	10^{19} – 10^{22} (in X-point 10^{20} – 10^{21})	$\delta n_e < 5\%$
T_e [eV]	0.3–100 (in X-point 100– 10^4)	$\delta T_e < 10\%$
T_i [eV]	0.3–100 (in X-point 100– 10^4)	$\delta T_i < 20\%$
$n_a(\text{H, D, T})$ [m^{-3}]	$>10^{16}$	$\delta n_a < 10\%$
$R_{\text{H/D}}; R_{\text{D/T}}$	0.1–10	$\delta R < 20\%$

diagnostic system should record data at a frequency from tens to hundreds of kilohertz. At the same time, this diagnostic system must work with laser operating in a burst mode. Such a system is probably the optimal solution for TRT, and similar systems have been successfully used at several tokamaks (see, for example, [6, 7]).

3. OPTICAL LAYOUT, LOCATION AT THE TOKAMAK, AND DIAGNOSTIC IMPLEMENTATION

The optical layout of the joint TS/LIF systems are built according to the classical scheme of laser diagnostics, which assumes the transverse arrangement of chords for probing and observation of scattered radiation (Figs. 2 and 3). The launchers of laser radiation are installed under the divertor cassettes. Laser chord 1, directed along the separatrix of the outer divertor leg, falls at an angle of approximately 5° onto the surface of the first wall (FW) element in row #1. Laser chord 2 (Fig. 3), directed along the outer divertor plate, ends on the back surface of the bend of the FW element in the row #10. Laser chord 3 (Fig. 2) crosses the region of the edge plasma (hereinafter, standardly referred to as SOL (scrape-off layer)) from the outside of X-point. Probing along chords 1 and 2 is supposed to be performed through the gap between neighboring divertor cassettes, and along chord 3, through the opening in center of the cassette in the TRT divertor port no. 13. The arrangement of probing chords 1 and 3 does not imply the use of laser dump. The laser dump for chord 2 can be situated on the back surface of the FW element of the row #10. Several directions of probing chords are supposed to be implemented using three different laser mirrors protected from contamination by thin quartz windows. The diagnostic laser beams of the TS and LIF diagnostics, operating at different wavelengths, are supposed to be matched using dielectric mirrors that reflect light in a narrow spectral range and are transparent at other wavelengths. The protective windows will be cleaned by radiation of power TS lasers (see, for example, [8]). For chord 3, the first laser mirror is most distant from the divertor plasma, and therefore, it is the most protected from contaminations. For chord 1, the solid angles for collecting scattered radiation and the projection of their optical axes onto the poloidal section are shown in Fig. 2.

3.1. TS Diagnostics

Spatial distributions of electron temperature T_e and plasma density n_e near divertor plates are characterized by steep gradients, extremely high density (up to $2 \times 10^{21} \text{ m}^{-3}$), and low temperatures ($\sim 0.3 \text{ eV}$ or somewhat higher). As we go away from the divertor plates and approach the X-point region, the changing of n_e and T_e become close to those typical of edge plasma in the

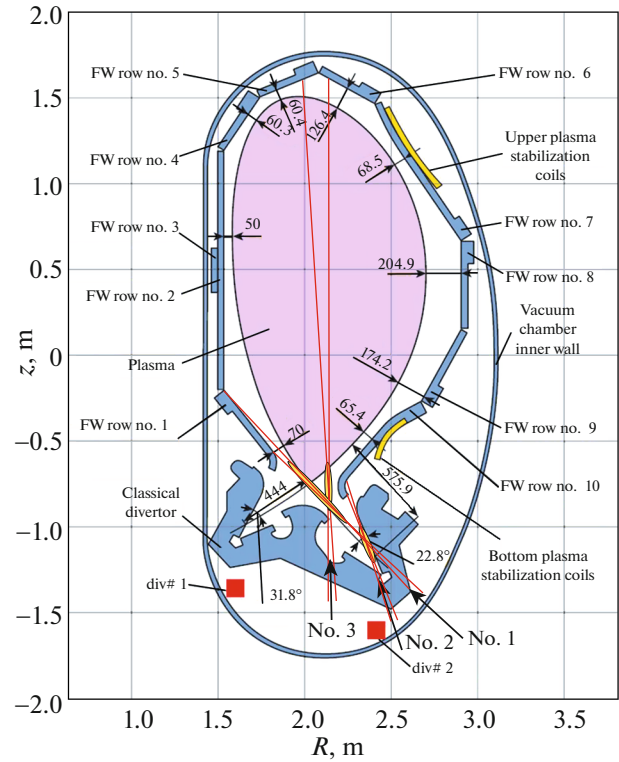


Fig. 1. Arrows nos. 1, 2, and 3 indicate directions of laser beams along plasma probing chords in the vicinity of X-point and along surface of outer divertor plate of joint TS/LIF laser diagnostics in divertor port no. 15. The figure shows numbering of the rows of first wall (FW) elements and their distances from plasma column. FW elements of rows nos. 1, 5, 6, and 10 will be exposed to laser radiation. Abbreviations div#1 and div#2 indicate positions of control coils located inside vacuum volume and limiting free space under divertor cassettes.

main vacuum chamber of tokamak. For plasma with high electron density and low electron temperature, Debye length becomes comparable to the laser wavelength, and deviation of the shape of TS spectra from Gaussian becomes very noticeable due to the collective scattering effects. Therefore, the standard algorithm for TS signal processing based on separation of the T_e and n_e variables (which is valid for light scattering by free electrons) becomes invalid, since the shape of TS spectrum becomes a function not only of the temperature T_e , but also of the density n_e . The influence of collective effects on the differential scattering cross section of laser radiation $\frac{d\sigma_\omega}{d\omega d\Phi}$ can be taken into account solving the following equations [9]:

$$\frac{d\sigma_\omega}{d\omega d\Phi} = \frac{e^4}{m^2 c^4 \sqrt{\pi}} \left[\frac{\Gamma_\alpha(x)}{\omega_e} + Z \left(\frac{\alpha^2}{1 + \alpha^2} \right)^2 \frac{\Gamma_\beta(y)}{\omega_i} \right], \quad (1)$$

where

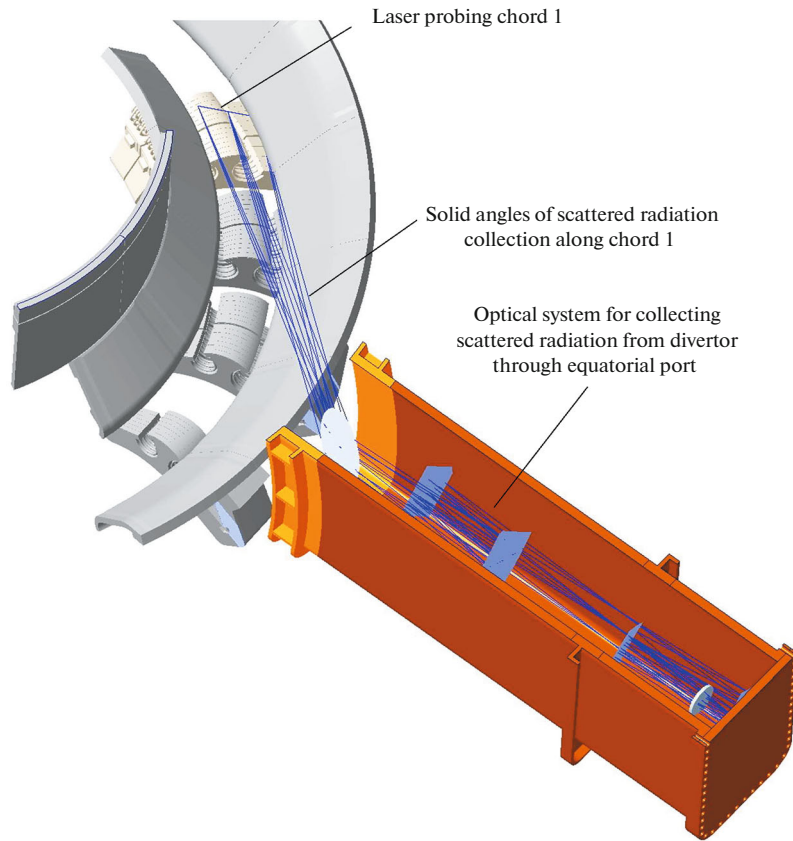


Fig. 2. Solid angles for collecting radiation scattered along laser chord 1. Optical system will also be used to collect radiation scattered along laser chord 3 (see Fig. 1).

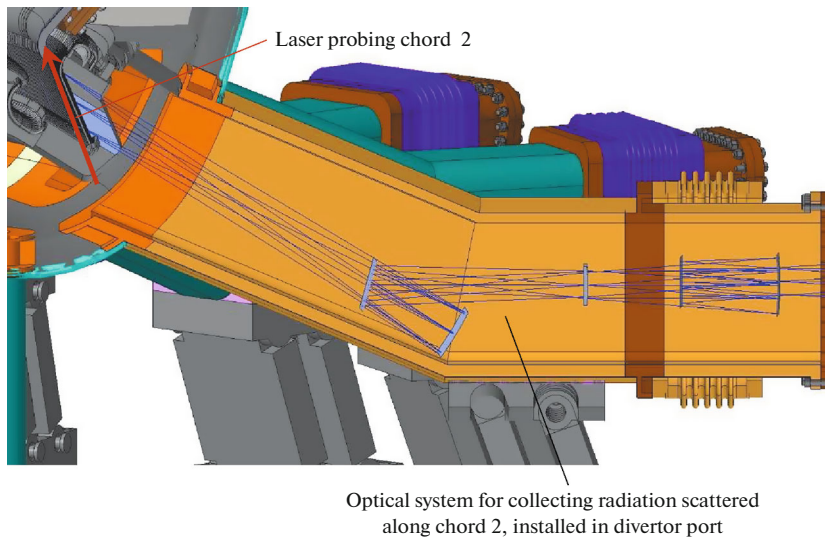


Fig. 3. Solid angles and mirror optical system for collecting radiation scattered along chord 2, installed in vacuum volume of diagnostic divertor port. Solid angles are shown to the end of vacuum flange of the divertor port (in figure on the right).

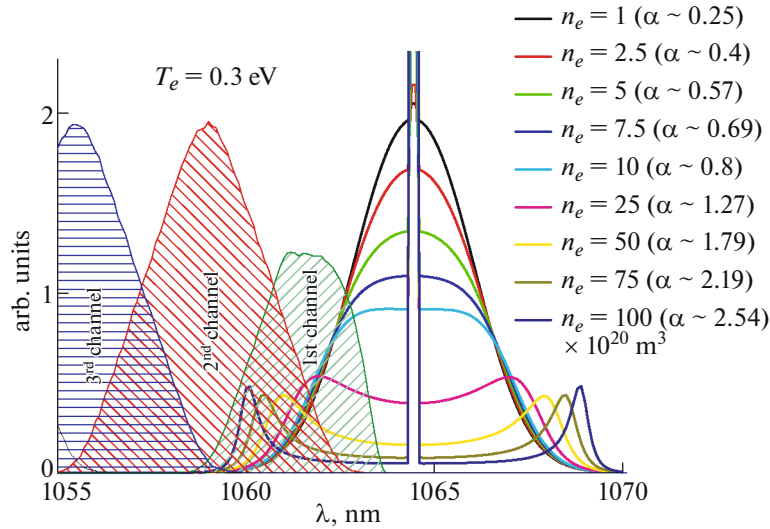


Fig. 4. Shapes of Thomson scattering spectra for $T_e = 0.3$ eV and changes in the Salpeter parameter α from 0.25 (at $n_e = 10^{20} \text{ m}^{-3}$) to 2.54 (at $n_e = 10^{22} \text{ m}^{-3}$). Shaded contours correspond to spectral transmissions of first three spectral channels of grating polychromator [5].

$$\Gamma_\alpha(x) = \frac{\exp(-x^2)}{\left[1 - \alpha^2 \left(2x \int_0^x \exp(t^2 - x^2) dt - 1\right)\right]^2 + \pi\alpha^4 x^2 \exp(-2x^2)},$$

$$x = \Omega/\omega_e; \quad y = \Omega/\omega_i; \quad \Omega = \omega - \omega_0,$$

ω and ω_0 are the frequencies of scattered and incident radiation, respectively;

$$\omega_e = \frac{2\omega}{c} \sqrt{\frac{2T_e}{m}} \sin\left(\frac{\theta}{2}\right); \quad \omega_i = \frac{2\omega}{c} \sqrt{\frac{2T_i}{M}} \sin\left(\frac{\theta}{2}\right),$$

$$\alpha = \frac{c}{\omega_0 \sin(\theta/2)} \sqrt{\frac{\pi n_e e^2}{T_e}}; \quad \beta^2 = Z \frac{T_e}{T_i} \frac{\alpha^2}{1 + \alpha^2},$$

c is the speed of light in vacuum, T_e and T_i are the electron and ion temperatures, respectively, Z is the ion charge, n_e is the electron density, m and M are the electron and ion masses, respectively, e is the electron charge, θ is the scattering angle, and Φ is the solid angle.

For the temperature $T_e = 0.3$ eV and the density n_e in the range from 10^{14} to 10^{16} m^{-3} , the shapes of TS spectra are shown in Fig. 4 together with the spectral curves of the first three spectral channels of the grating polychromator. For the TS diagnostics, within this range of plasma density, the corresponding Salpeter parameter varies from 0.25 to 2.54.

For the TS spectra with considerable contribution of collective effects, it is proposed to estimate the expected measurement errors of the electron density n_e and temperature T_e using the following algorithm [10]:

(a) estimation of the TS signals in spectral channels based on known technical parameters using the shape of TS spectra calculated in accordance with equation (1);

(b) manifold solution (e.g., 10^3 times) of the inverse problem of recovering the T_e and n_e parameters from the simulated TS signals for given n_e and T_e parameters with allowance for random deviations $\sigma_{N_i} = \sqrt{k(N_i + 2N_{\text{bg}i}) + 2N_{\text{amp}}^2}$. Here, $k \sim 2.5$ is the excess noise of detector, N_i and $N_{\text{bg}i}$ are the numbers of photoelectrons in desired and background signals in the i -th spectral channel, respectively, and N_{amp} is the noise of detector, including subsequent amplification, recalculated into the number of photoelectrons at the input (~ 5 – 10 photoelectrons) [11];

(c) estimation of standard deviations based on the obtained distributions of the T_e and n_e parameters.

3.2. LIF Diagnostics

The use of laser-induced fluorescence (LIF) diagnostics, which measures emission of highly excited levels, requires knowledge of the n_e and T_e parameters to calculate population of the excited levels. Particularly critical is accuracy of knowing parameters of electron component for the region of turbulent divertor plasma under study, which is characterized by strong inhomogeneity. When the LIF diagnostic being developed is combined with the TS diagnostics, the measurements of both diagnostics are performed at the same points. The LIF diagnostics is planned to be used for measuring ion temperature T_i in divertor by means of analyzing emission of singly ionized helium

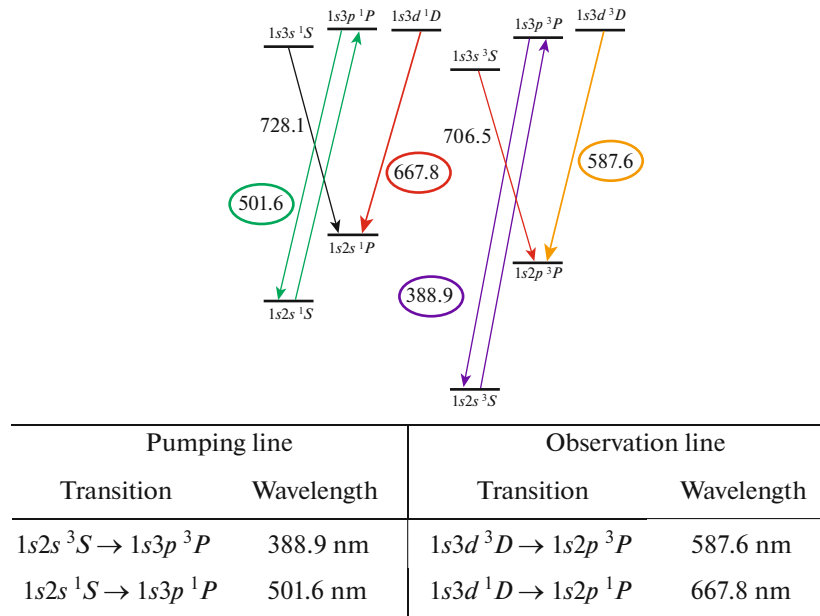


Fig. 5. Scheme of transitions of helium atom and proposed pairs of lines that can be used to measure density of atomic helium n_{HeI} using the LIF method.

ion HeII. Detailed description of the method is given in [12]. The scheme of radiative transitions in helium atom, including the pairs of transitions that can be used for plasma diagnostics, is shown in Fig. 5.

For the helium ion diagnostics, it is proposed to use the laser-induced fluorescence quenching (LIQ) technique with quenching of the 468.6 nm line (transition $n = 4 \rightarrow 3$), which is the most intense in visible range (see Fig. 6). Information on Doppler width of the line contour can be obtained by means of scanning spectral line with a narrow-band laser. For quenching 468.6 nm line, it is proposed to use transition from the level with the lowest principal quantum number n in the transition $n = 4 \rightarrow 5$ (1012.3 nm), in order to minimize the effect of Stark broadening. In addition to Doppler broadening, this technique must take into account Zeeman and Stark broadenings of the spectral line, which affect width of the emission line.

Another diagnostics using the LIQ principle is the diagnostics of atomic emission of hydrogen isotopes. Information about distribution of hydrogen atoms in edge plasma of tokamak is of great importance. The process of hydrogen isotope recycling from the first wall is of great importance in the case of increasing duration of discharge in tokamak. In particular, the LIQ diagnostics can indicate reaching stationary state of hydrogen flow from wall into the plasma or the efficiencies of the operating modes of tokamak-reactor with zero recycling walls, which are discussed in connection with the possible use of lithium technologies. In contrast to passive spectroscopy traditionally used for such measurements, the development and approbation of this method for measuring density of hydro-

gen atoms [2] will provide information necessary for studying processes in edge and divertor plasmas of tokamak. The diagnostics for hydrogen isotope atoms recently proposed is based on the laser-induced fluorescence quenching of the most intense lines of Balmer series. The quenching occurs as a result of transitions between levels with principal quantum numbers $n = 3 \rightarrow 2$ after laser excitation from level $n = 3$ to one of the higher ones ($n \geq 4$). For quenching of the lines of protium H_α ($\lambda_{\text{H}} = 656.28$ nm), deuterium D_α ($\lambda_{\text{D}} = 656.10$ nm), and tritium T_α ($\lambda_{\text{T}} = 656.04$ nm) (the corresponding differences in wavelengths are $\Delta(\lambda_{\text{H}} - \lambda_{\text{D}}) = 0.18$ nm and $\Delta(\lambda_{\text{D}} - \lambda_{\text{T}}) = 0.06$ nm), it is proposed to use the transition $n = 3 \rightarrow 4$ (1875.1 nm). The scheme of transitions of hydrogen atom is shown in Fig. 6.

4. CALIBRATION TECHNIQUES

One of the technical obstacles on the way to implementation of the optical diagnostics in fusion reactors is distortion of spectral characteristics, as well as absolute transmission, of the diagnostic optical system due to radiation-induced absorption and/or contamination of optical elements with erosion products of the first wall. During operation of the tokamak with reactor technologies, it is difficult to regularly calibrate the absolute transmission of optical windows as well as distortion of their spectral transmission. The absolute transmission affects measurements of plasma density n_e , helium density $n_a(\text{He})$, and hydrogen isotope density $n_a(\text{H}, \text{D}, \text{T})$, and the spectral distortion affects measurements of electron temperature T_e . Therefore,

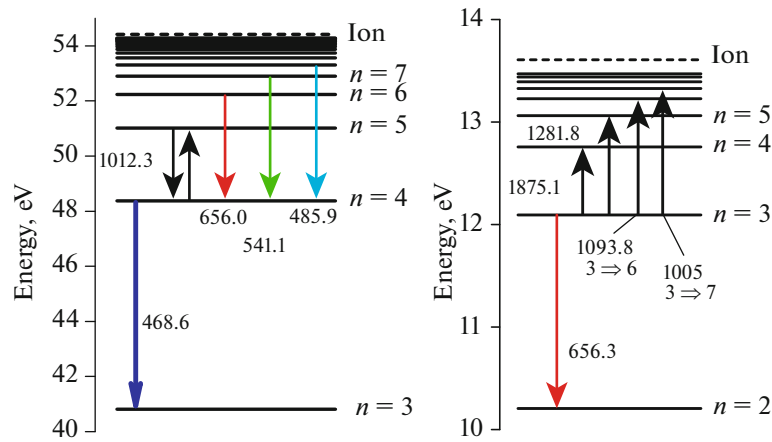


Fig. 6. Schemes of transitions of singly ionized helium ion (left) and hydrogen atom (right).

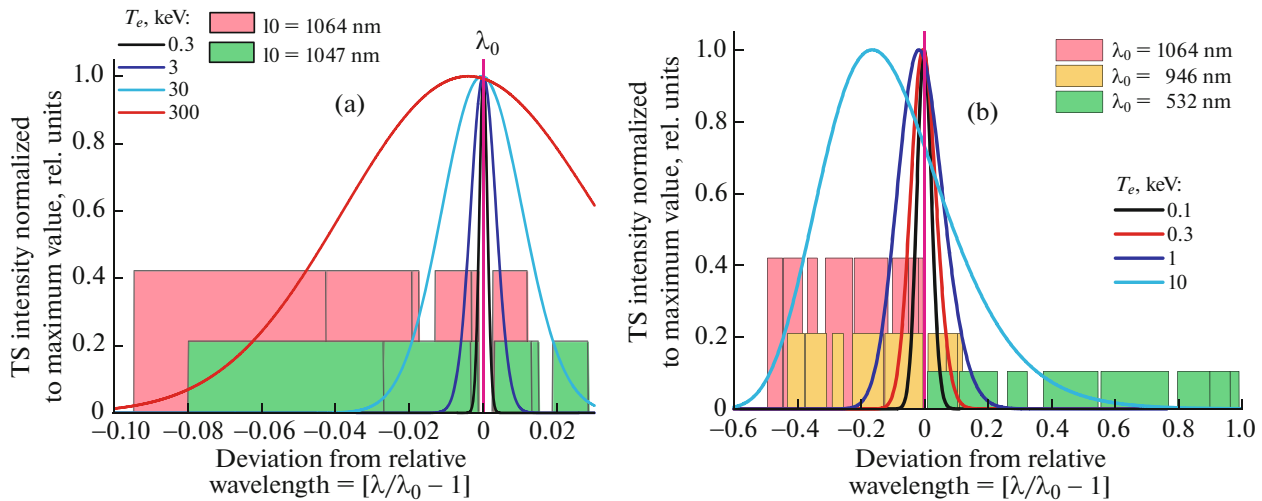


Fig. 7. Positions of transmission curves of polychromator spectral channels of TS system and contours of Thomson scattering lines. Transmissions of spectral channels at different laser wavelengths are shown by rectangles of different heights. (a) Relative positions of the set of spectral channels and Thomson contours of lines for wavelengths of 1064 and 1047 nm and electron temperatures of 0.3, 3, 30, and 300 eV and (b) relative positions of the set of spectral channels and Thomson contours of lines for wavelengths of 1064, 946, and 532 nm and electron temperatures of 0.1, 1, 10, and 25 keV.

reliability of the data of laser diagnostics of divertor plasma will decrease with time.

4.1. Calibration of Spectral Transmission of Optical System

To calibrate the spectral transmission of optical system, it is proposed to use TS with probing at several wavelengths [5]. For example, the transmission characteristics of polychromator spectral channels in the TS system and the Thomson scattering contours are shown in Fig. 7a for the case of studying plasma with temperatures from 0.3 to 300 eV near the divertor plate with the use of probing at wavelengths 1064 and 1047 nm. Similar characteristic are shown in Fig. 7b for the case of studying plasma with temperatures from 100 eV

up to 10 keV in the vicinity of X-point for probing at the wavelengths of Nd:YAG lasers of 1064, 946, and 532 nm.

4.2. Calibration of Absolute Transmission of Optical System

The routine approach to absolute calibration of the optical system transmission of TS diagnostics requires periodic puffing gas into the vacuum chamber and performing calibration using Raman or Rayleigh scattering. Transition to the stationary burning regime will require the use of other technologies. In core plasma, the density n_e can be controlled by means of comparing the measured density profiles with chord-averaged measurements performed by interferometer, while for

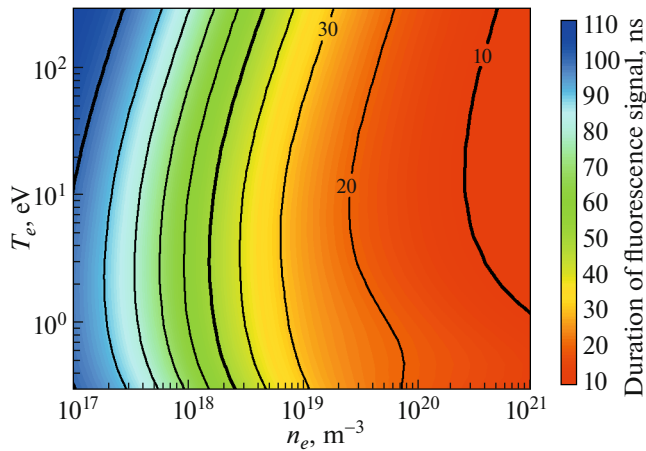


Fig. 8. Duration of fluorescence signal at the wavelength of helium atom He I 587.6 nm as a function of plasma density n_e and electron temperature T_e in the case of excitation by laser with wavelength of 388.9 nm at the following characteristics of laser pulse: pulse duration is 10 ns, pulse energy is 1 mJ, laser line width is $\Delta\lambda = 50$ pm, and laser beam cross section is 1 cm^2 [2].

measuring the density n_e in divertor, it is proposed to use temporal variation of HeI fluorescence signals [13]. For example, the plasma density n_e can be reliably measured in the range of 10^{17} – 10^{21} m^{-3} for the temperature range of $T_e = 0.3$ – 200 eV in the case of exciting the line 388.9 nm ($1s2s^3S \rightarrow 1s3p^3P$) using a pulsed laser with duration of 10 ns, energy of 1 mJ, spectral width of 1000 pm, and laser beam cross section of 1 cm^2 (see Fig. 8).

5. CONCLUSIONS

The combined laser diagnostic for measuring plasma parameters in divertor and in X-point region has been proposed for use at the TRT facility. The approach is based on joint laser diagnostics of Thomson scattering and laser-induced fluorescence. It is proposed to perform measurements along three laser chords launched into the plasma through the TRT divertor port no. 15. The collection optical systems are proposed to be located in divertor port no. 15 and equatorial port no. 13. Each of the laser probing chords has its own functional task. The probing chord launched along the outer divertor target has to measure the heat load distribution over the outer divertor plate, as well as the position and width of the strike point region. The chord directed along separatrix can be used to measure gradients of electron, ion, and neutral plasma components in the region from strike point up to X-point region. The probing chord directed vertically from under the divertor cassette will be used to measure plasma parameters in the vicinity of X-point at the divertor entrance.

The set of parameters measured by the joint TS/LIF diagnostics can be used for:

- controlling divertor operation modes by means of localization of regions with preferential ionization/recombination; this will be done by means of measuring the local ionization and recombination rates (T_e , n_e , and $n_a(\text{He, H, D, T})$);

- calculating friction forces in plasma flows against neutral components (T_i , n_i , and $n_a(\text{He, H, D, T})$) at known velocity of relative motion of the plasma components;

- calculating changes in pressures of the plasma components along the outer leg of divertor ($T_e n_e$, $T_i n_i$);

- determining isotopic ratios $R_{\text{H/D}}$ and $R_{\text{D/T}}$ for hydrogen isotopes.

FUNDING

The formulation of the problems that can be solved with the help of TS diagnostics, as well as formulation of the technical requirements for TS system (Sections 1 and 2), were supported by the Ministry of Science and Education of the Russian Federation under the State Contract no. 0040-2019-0023. The working out of the schemes for placing the diagnostics at the tokamak, as well as the analysis of the expected measurement accuracy and development of the approaches to diagnostics calibration (Sections 3 and 4), were supported by the Ministry of Education and Science of the Russian Federation under the State Contract no. 0034-2019-0001.

CONFLICT OF INTEREST

The authors declare that they have no conflicts of interest.

REFERENCES

1. S. Krashenninnikov, A. Smolyakov, and A. Kukushkin, *On the Edge of Magnetic Fusion Devices. (Springer Series in Plasma Science and Technology)* (Springer Nature Switzerland, Cham, 2020).
2. E. E. Mukhin, G. S. Kurskiev, A. V. Gorbunov, D. S. Samsonov, S. Yu. Tolstyakov, A. G. Razdobarin, N. A. Babinov, A. N. Bazhenov, I. M. Bukreev, A. M. Dmitriev, D. I. Elets, A. N. Koval, A. E. Litvinov, S. V. Masyukevich, V. A. Senitchenkov, et al., *Nucl. Fusion* **59**, 086052 (2019). <https://doi.org/10.1088/1741-4326/ab1cd5>
3. R. A. Pitts, X. Bonnin, F. Escourbiac, H. Frerichs, J. P. Gunn, T. Hirai, A. S. Kukushkin, E. Kaveeva, M. A. Miller, D. Moulton, V. Rozhansky, I. Senichenkov, E. Sytova, O. Schmitz, P. C. Stangeby, et al., *Nucl. Mater. Energy* **20**, 100696 (2019). <https://doi.org/10.1016/j.nme.2019.100696>
4. R. A. Pitts, P. Andrew, G. Arnoux, T. Eich, W. Fundamenski, A. Huber, C. Silva, D. Tskhakaya, and JET EFDA Contributors, *Nucl. Fusion* **47**, 1437 (2007). <https://doi.org/10.1088/0029-5515/47/11/005>

5. E. E. Mukhin, R. A. Pitts, P. Andrew, I. M. Bukreev, P. V. Chernakov, L. Giudicotti, G. Huijsmans, M. M. Kochergin, A. N. Koval, A. S. Kukushkin, G. S. Kurskiev, A. E. Litvinov, S. V. Masyukevich, R. Pasqualotto, A. G. Razdobarin, et al., *Nucl. Fusion* **54**, 043007 (2014).
<https://doi.org/10.1088/0029-5515/54/4/043007>
6. D. J. Den Hartog, J. R. Ambuel, M. T. Borchardt, A. F. Falkowski, W. S. Harris, D. J. Holly, E. Parke, J. A. Reusch, P. E. Robl, H. D. Stephens, and Y. M. Yang, *Rev. Sci. Instrum.* **81**, 10D513 (2010).
<https://doi.org/10.1063/1.3475723>
7. R. Scannell, M. J. Walsh, P. G. Carolan, N. J. Conway, A. C. Darke, M. R. Dunstan, D. Hare, and S. L. Prunty, *Rev. Sci. Instrum.* **77**, 10E510 (2006).
<https://doi.org/10.1063/1.2237488>
8. B. W. Brown, C. W. Gowers, P. Nielsen, and B. Schunke, *Rev. Sci. Instrum.* **66**, 3077 (1995).
<https://doi.org/10.1063/1.1145534>
9. D. Evans and J. Katzenstein, *Rep. Prog. Phys.* **32**, 207 (1969).
<https://doi.org/10.1088/0034-4885/32/1/305>
10. G. S. Kurskiev, P. A. Sdvizhenskii, M. Bassan, P. Andrew, A. N. Bazhenov, I. M. Bukreev, P. V. Chernakov, M. M. Kochergin, A. B. Kukushkin, A. S. Kukushkin, E. E. Mukhin, A. G. Razdobarin, D. S. Samsonov, V. V. Semenov, S. Yu. Tolstyakov, et al., *Nucl. Fusion* **55**, 053024 (2015).
<https://doi.org/10.1088/0029-5515/55/5/053024>
11. N. S. Zhiltsov, G. S. Kurskiev, E. E. Mukhin, V. A. Solovey, S. Yu. Tolstyakov, S. E. Aleksandrov, A. N. Bazhenov, and Al. P. Chernakov, *Nucl. Instrum. Methods Phys. Res., Sect. A* **976**, 164289 (2020).
<https://doi.org/10.1016/j.nima.2020.164289>
12. A. V. Gorbunov, E. E. Mukhin, E. B. Berik, K. Yu. Vukolov, V. S. Lisitsa, A. S. Kukushkin, M. G. Levashova, R. Barnsley, G. Vayakis, and M. J. Walsh, *Fusion Eng. Des.* **123**, 695 (2017).
<https://doi.org/10.1016/j.fusengdes.2017.05.129>
13. A. Gorbunov, D. A. Shuvaev, and I. V. Moskalenko, *Plasma Phys. Rep.* **38**, 574 (2012).
<https://doi.org/10.1134/S1063780X12070021>

Translated by I. Grishina